Segmentation of Left Ventricle in Cardiac Cine MRI: An Automatic Image-Driven Method

YingLi Lu[1], Perry Radau[1], Kim Connelly[1,2], Alexander Dick[3], and Graham A. Wright[1]

[1] Imaging Research, Sunnybrook Health Sciences Centre, Toronto, ON, Canada
[2] Cardiology, St Michael's Hospital, Toronto, ON, Canada
[3] Cardiology, Sunnybrook Health Sciences Centre, Toronto, ON, Canada
yinglilu@gmail.com, perry.radau@gmail.com, connellyka@yahoo.ca, Alexander.Dick@sunnybrook.ca, gawright@sten.sunnybrook.utoronto.ca

Abstract. This study investigates a fully automatic left ventricle segmentation method from cine short axis MR images. Advantages of this method include that it: 1) does not require manually drawn initial contours, trained statistical shape or gray-level appearance model; 2) provides not only endocardial and epicardial contours, but also papillary muscles and trabeculations' contours; 3) introduces a roundness measure that is fast and automatically locates the left ventricle; 4) simplifies the epicardial contour segmentation by mapping the pixels from Cartesian to approximately polar coordinates; and 5) applies a fast Fourier transform to smooth the endocardial and epicardial contours. Quantitative evaluation was performed on 41 subjects. The average perpendicular distance between manually drawn and automatically selected contours over all slices, all studies, and two phases (end-diastole and end-systole) was 1.40 ± 1.18 mm for endocardial and 1.75 ± 1.15 mm for epicardial contours. These results indicate a promising method for automatic segmentation of left ventricle for clinical use.

Keywords: Cardiac, left ventricle, segmentation, MRI.

1 Introduction

To quantitatively analyze global and regional cardiac function from cine magnetic resonance (MR) images, clinical parameters such as ejection fraction (EF), left ventricle volume, peak ejection rate, and filling rate are required. Calculations of these parameters depend upon accurate delineation of endocardial and epicardial contours of the left ventricle (LV). Manual delineation is time-consuming and tedious and has high inter-observer variability. Moreover, in clinical practice the manual delineation is typically limited to the end-diastolic (ED) and end-systolic (ES) phases, which can not be used to compute the peak ejection and filling rates. Thus, fully automatic LV segmentation on all of the phases is desirable.

The automatic segmentation of the LV in cine MR typically faces four challenges: 1) the overlap between the intensity distributions within the cardiac regions; 2) the lack of edge information; 3) the shape variability of the endocardial and epicardial

N. Ayache, H. Delingette, and M. Sermesant (Eds.): FIMH 2009, LNCS 5528, pp. 339–347, 2009.

contours across slices and phases; and 4) the inter-subject variability of 1), 2) and 3). A number of methods have been proposed for (semi-) automatic LV segmentation, including using a probability atlas [1], dynamic programming [2-3], fuzzy clustering [4], a deformable model [5], an active appearance model [6], a variational and level set [7-10], graph cuts [11-12] and an image-driven approach [13]. For a complete review of recent literature describing cardiac segmentation techniques, see [14]. Although the segmentation results have improved, accurate LV segmentation is still acknowledged as a difficult problem.

In this work, we investigated a novel image-driven method for the accurate, robust, and fully automatic LV segmentation from short axis (SAX) cine MR images. The method is expected to give accurate segmentation of papillary and trabecular muscles, as well as endocardial and epicardial contours in all the phases. Main contributions of the work are that it: 1) introduces a roundness-measure-based fast and automatic LV location technique; 2) simplifies the epicardial contours segmentation by mapping the pixels from Cartesian to approximately polar coordinates; and 3) applies a fast Fourier transform to smooth the endocardial and epicardial contours.

2 Materials and Methods

2.1 Datasets

For this study, data from 41 patients were analyzed (8 female, 33 male; age: 60.3 ± 12.2). Cine steady state free precession (SSFP) MR short axis (SAX) images were obtained with a 1.5T GE Signa MRI. All the images were obtained during 10-15 second breath-holds with a temporal resolution of 20 cardiac phases over the heart cycle, and scanned from the ED phase. Six to 12 SAX images were obtained from the atrioventricular ring to the apex (thickness=8mm, gap=8mm, FOV=320mm$\times$ 320mm, matrix= 256×256). In these SAX MR acquisitions, endocardial and epicardial contours were drawn by a cardiologist in all slices at ED and ES phases, following the convention of including papillary muscles and endocardial trabeculations in the ventricular cavity. These manually drawn contours were used as the "gold standard" for evaluation purposes.

2.2 LV Location

This section presents method based on a roundness metric to automatically locate the LV blood pool's centroid on the middle slice in the ED phase. This method is based on the following assumptions: 1) the heart is approximately in the centre of the original image; 2) the left ventricle blood pool is more circular than the right ventricle blood pool; and 3) the blood has higher signal intensity than the myocardium (i.e., bright blood imaging). This procedure consists of five steps (refer to Fig.1):

1. Choose the middle (normally in the mid-cavity level) slice image in the ED phase as the target image.
2. Specify a centered, fixed rectangular region of interest (ROI) on the target image. The size of the rectangular is 110$\times$ 110pixels (Fig.1a, b).

3. Apply the optimal threshold method of Otsu[15] to convert the ROI to a binary image (Fig.1c).
4. Remove all objects smaller than a predefined threshold (40 pixels) and compute the convex hull of the surviving objects (Fig.1d).
5. Compute the roundness metric $R = \frac{4\pi A}{P^2}$ of each survived convex-hulled object, where, A is area and P is perimeter length. R is equal to 1 for a circle. The object with the largest roundness metric is recognized as the LV blood pool, and its centroid coordinate (x, y) is utilized for following segmentation (Fig.1d).

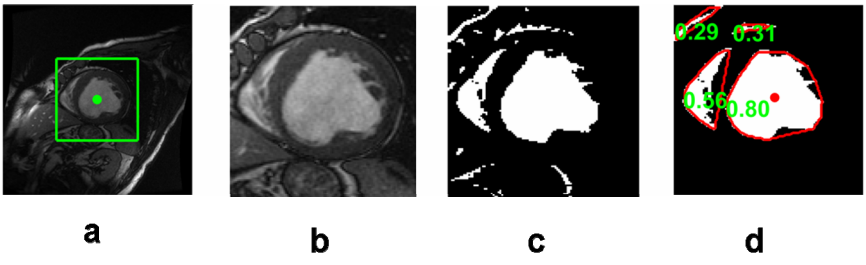

Fig. 1. LV location procedure. (a) Target image with rectangular ROI (green box) and image center(green point), (b) ROI image, (c) Binary image, (d) Surviving objects' convex hulls (red) and the corresponding roundness metric(green). The detected LV blood pool centroid is labeled as a red point.

2.3 LV Segmentation

For each 2D image, the LV blood pool contour, endocardial contour, papillary muscles' and trabeculations' contours, and epicardial contour will be detected sequentially. Given a 2D image, the first problem is how to specify a ROI that includes the LV. Our method uses a fixed size rectangle centered on the predetermined centroid (x, y) of the LV blood pool to determine an ROI. This is based on the assumption that the central part of the LV blood pool does not move much across slices and phases.

The blood pool contour is detected by the following steps (refer to Fig.2a-g):

1. Specify a rectangular ROI centered on the previously identified LV blood pool centroid coordinate (x, y) (see Section 2.2). The size of the rectangle is 110×110pixels (Fig.2a, b);
2. Apply the optimal threshold method of Otsu[15] to convert the ROI to a binary image (Fig.2c);
3. The LV blood pool object is identified by choosing the object that has maximum overlap with a predefined mask (20×20 pixels) centered on the LV blood pool centroid (Fig.2d);
4. Dilate the LV blood pool object by a disk-shaped structuring element with radius of 20 pixels to produce a refined, smaller ROI (Fig.2e);
5. Repeat steps 2-3 based on the refined ROI. This will give a refined blood pool mask (Fig.2f).

The endocardial contour is detected by the following steps (refer to Fig.2h, i):

1. Compute the convex hull of the refined blood pool (Fig.2h);
2. Smooth the convex hull's contour by applying the 1D fast Fourier transform (FFT) [16]. We first compute the FFT of the x coordinate of the contour point index, multiply the result by a low pass filter transfer function (keep only the four lowest frequency components), then take the inverse transform to produce the smoothed x coordinate. Repeat for y coordinates (Fig.2i).

The papillary muscles' and trabeculations' contours are detected by these steps:

1. Subtract the convex-hull mask of the refined blood pool from the refined blood pool mask to calculate the mask image of the papillary muscles and trabeculations (Fig.2j);
2. Trace the exterior boundaries of the objects in the mask image to determine the papillary muscles' and trabeculations' contours (Fig.2k).

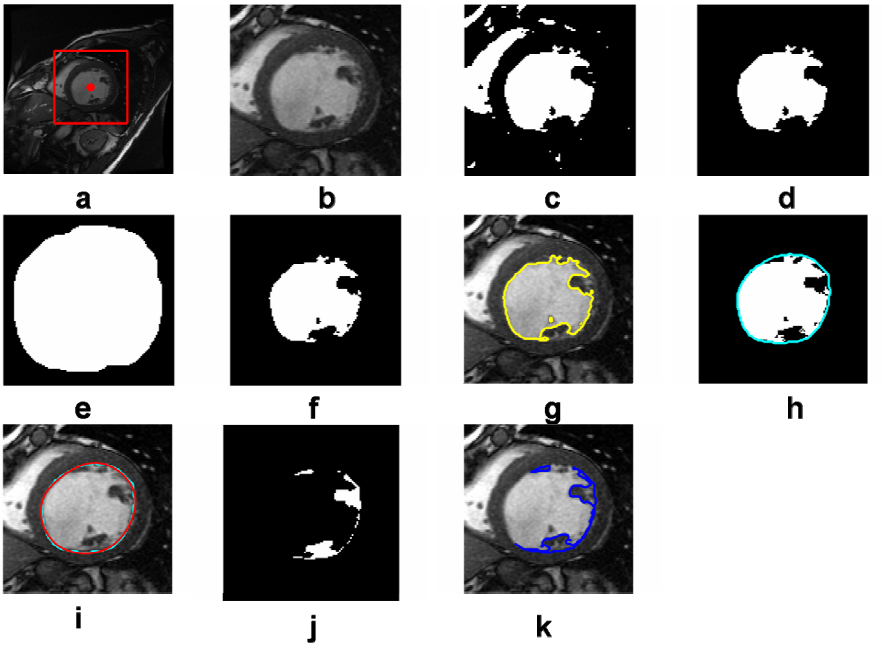

Fig. 2. LV contour calculation procedure. (a) Image with rectangular ROI and previously identified LV blood pool centroid (red), (b) ROI image, (c) Binary image, (d) Coarse LV blood pool, (e) Dilated mask, (f) Refined LV blood pool, (g) LV blood pool contour, (h) Convex hull of the LV blood pool (cyan), (i) Smoothed endocardial contour (red), (j) Papillary muscles and trabeculations' mask, (k) Papillary muscles and trabeculations' contours (blue).

The epicardial contour is calculated by the following steps (refer to Fig.3a-f):

1. Map the pixels from Cartesian to approximately polar coordinates. An outer boundary is calculated by dilation of the endocardial contour. The two contours

are interpolated to the same number of points, and paired to derive scan lines, each of a predefined length (20 pixels) (Fig. 3a). The result is a rectangular image that extends from the endocardial contour (top row) outward (bottom row) (Fig.3b).

2. Use each top-row pixel as a region growing seed, with all grown regions added and converted to a binary image (Fig.3c). For region growing, intensities are normalized by the original image maximum, and pixels added to a grown region must meet the intensity criterion (difference from mean of the grown region less than 0.04).
3. Fill image holes by morphological operations (Fig.3d).
4. The end point of each column's grown region determines an edge point (Fig.3e).
5. Inverse transform the edge point coordinates to the original coordinate space to determine the epicardial contour (Fig.3f).
6. Smooth the contour by applying the FFT technique as described earlier (Fig.3f).

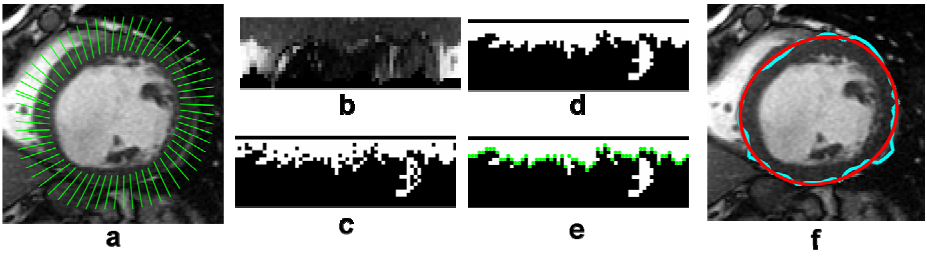

Fig. 3. LV segmentation procedure for epicardial contour. (a) Scan lines for mapping the pixels from Cartesian to polar coordinates. (b) Result of image transform. (c) Region growing binary image. (d) Image after filling holes. (e) Edge points (green). (f) Epicardial contour before (blue) and after FFT smoothing (red).

2.4 Evaluation

In order to quantitatively evaluate the automatically detected endocardial and epicardial contours of the ED and ES phases of all slices, three quantitative measures were assessed. First, the average perpendicular distance measures the distance from the automatically segmented contour to the corresponding manually drawn expert contour, averaged over all contour points. Second, the Dice metric [8]

$$DM = 2A_{am}(A_a + A_m)^{-1}$$

is a measure of contour overlap utilizing the contour areas automatically segmented (A_a), manually segmented (A_m), and their intersection (A_{am}). *DM* is always between 0 and 1, with higher *DM* indicating better match between automatic and manual segmentations. Third, the ejection fractions determined by the manual and automatic methods were compared by correlation analysis. In addition, the average perpendicular distance and Dice metric were compared with those calculated for a commercial automatic segmentation technique (Qmass MR 6.2.3, Medis[17]).

3 Results

The automatic segmentation methods were tested on 41 clinical MR exams. The averaged perpendicular distance and Dice metric over all subjects and slices in the ED and ES phases calculated for our method and QMass are shown in Tables 1 and 2. The automatically determined ejection fractions were highly correlated (0.95) with those from manual contours. Representative results for one dataset are shown in Fig. 4. Note that the segmentation method failed on three images because those images included the valve joining the atrium and ventricle.

Table 1. Averaged perpendicular distances (mm)

	QMass	Our Method
Endocardial Contour	1.75 ± 1.13	1.40 ± 1.18
Epicardial Contour	4.11 ± 2.72	1.67 ± 1.15

Table 2. Dice metric

	QMass	Our Method
Cavity Area	0.92 ± 0.07	0.93 ± 0.06
Epicardial area	0.89 ± 0.08	0.95 ± 0.04

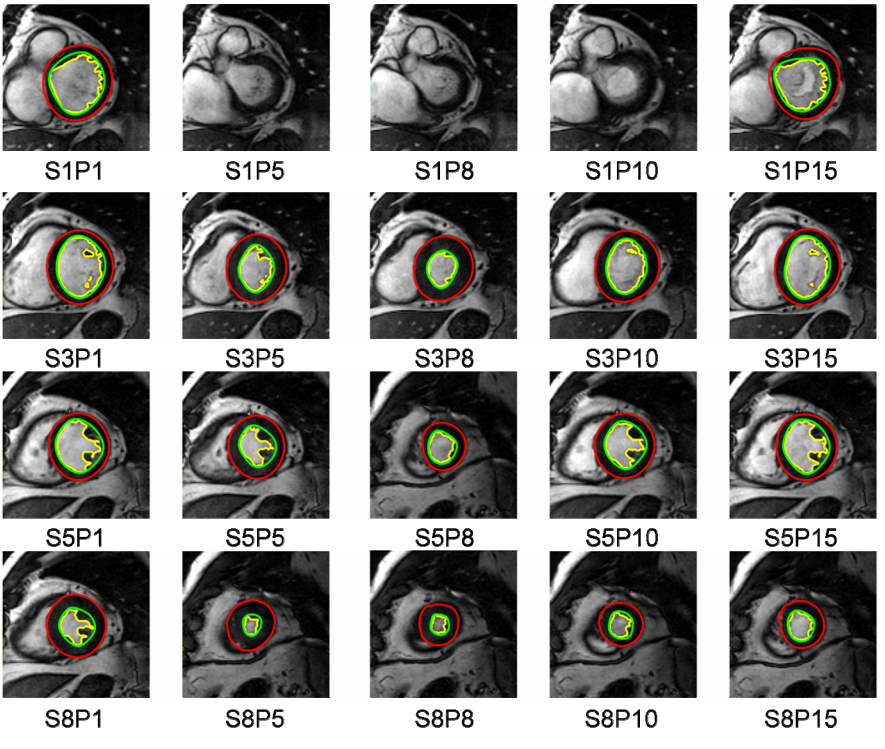

Fig. 4. Representative segmentation results. SxPy indicates the image for slice x and phase y. The contours of the blood pool (yellow), endocardium (green), and epicardium (red) are shown.

The average computation time of LV location is 0.085 ± 0.013s per subject. The average computation time of the segmentation of the proposed method is 53.7 ± 14.0s per subject (8 slices, 20 phases). The computation time was tested on consumer hardware (2×2.8GHz Quad-core Intel Xeon Mac Pro, Apple) with a non-optimized Matlab code (Mathworks) implementation.

4 Discussion and Conclusions

The proposed method for automatic segmentation has good accuracy, and was found to be superior in direct comparison with the automated technique of QMass. For further comparison, the perpendicular distance evaluations from other recent LV segmentation methods are provided in Table 3. Although dataset specifics are not uniform and thus hinder direct comparison, this meta-analysis provides additional confidence in our method.

Table 3. Averaged perpendicular distances (mm) of recent reported results

	Lorenzo-Valdés M.[1]	Uzümcü M.[3]	Fradkin M.[9]	Van Assen H.C.[18]	Our Method
Endocardial Contour	1.88	1.86	1.27	1.97	1.40
Epicardial Contour	2.75	1.77	1.56	2.23	1.67

The proposed segmentation method does not need initialization by manually drawn contours, prior statistical shape model, or gray-level appearance model. The proposed method is an image-driven method with only the assumption that the LV blood pool in a short axis image is approximately circular. Therefore it should be suitable for datasets with a wide range of anatomy, function, and image contrast as required for routine clinical use.

Previous methods of LV location have two steps: locate the entire heart and then the LV. For instance, standard deviation of the pixel values [19] and FFT based average and first harmonic magnitude image methods [22] have been used to locate the heart, and the Hough transformation [2, 6] has been proposed to locate the LV by detecting the circular region in the heart ROI. The proposed roundness metric method provides another available option for locating LV. And, it is very fast, requiring only 0.085 ± 0.013s per subject.

A difficult challenge of LV segmentation is the accurate delineation of the epicardial contours. The typical problem is ballooning epicardial contours at the junction between myocardium and lung parenchyma and subdiaphragmatic tissues. The main reason is the small intensity difference between these tissues. By mapping the pixels from Cartesian to polar coordinates, the irregular, ring-shaped ROIs are transformed to rectangular images. In this way, the epicardial contour detection problem was simplified.

Smoothing the contours by the FFT is a very fast and effective technique. The main merit of the FFT technique is to provide smoothed contours by removing outliers of the detected edge points without changing the overall shape.

The proposed method can provide contours of papillary muscles and trabeculations. Clinical studies have employed different quantification methods for calculation of LV volume, mass and ejection fraction by including or excluding

papillary muscles and trabeculations in the ventricular cavity [20, 21]. Recent studies have shown that the papillary muscles and trabeculations have a significant impact on calculation of LV volume and mass [20] and ejection fraction [21]; therefore the proposed method provides additional important options for daily clinical application.

A limitation of the proposed method is that it can not segment the LV from the right ventricle if the SAX slice includes the atria, as indicated in Fig. 4. Future research will extend the algorithm to handle these cases.

Future work will include testing the robustness of the algorithm with images acquired with different pulse sequences, contrast, and SNR characteristics, to validate our preliminary evidence of robustness. In addition, further evaluation is required with a spectrum of pathologies including ischemic and non-ischemic heart failure cases, and hypertrophic cases.

In summary, the proposed fully automated segmentation technique is fast, accurate and robust and should be of benefit for quantification of cine cardiac MR in clinical practice.

References

1. Lorenzo-Valdés, M., Sanchez-Ortiz, G.I., Elkington, A.G., Mohiaddin, R.H., Rueckert, D.: Segmentation of 4D cardiac MR images using a probabilistic atlas and the EM algorithm. Med. Image Anal. 8(3), 255–265 (2004)
2. Pednekar, A., Kurkure, U., Muthupillai, R., Flamm, S., Kakadiaris, I.A.: Automated left ventricular segmentation in cardiac MRI. IEEE Trans. Biomed. Eng. 53(7), 1425–1428 (2006)
3. Uzümcü, M., van der Geest, R.J., Swingen, C., Reiber, J.H., Lelieveldt, B.P.: Time continuous tracking and segmentation of cardiovascular magnetic resonance images using multidimensional dynamic programming. Invest. Radiol. 41(1), 52–62 (2006)
4. Rezaee, M.R., van der Zwet, P.J., Lelieveldt, B.E., van der Geest, R.J., Reiber, J.C.: A multi-resolution image segmentation technique based on pyramidal segmentation and fuzzy clustering. IEEE Trans. Image Process 9(7), 1238–1248 (2000)
5. Kaus, M.R., von Berg, J., Weese, J., Niessen, W., Pekar, V.: Automated segmentation of the left ventricle in cardiac MRI. Med. Image Anal. 8(3), 245–254 (2004)
6. Mitchell, S.C., Lelieveldt, B.P., van der Geest, R.J., Bosch, H.G., Reiber, J.H., Sonka, M.: Multistage hybrid active appearance model matching: segmentation of left and right ventricles in cardiac MR images. IEEE Trans. Med. Imaging 20(5), 415–423 (2001)
7. Paragios, N.: A level set approach for shape-driven segmentation and tracking of the left ventricle. IEEE Trans. Med. Imaging 22(6), 773–776 (2003)
8. Lynch, M., Ghita, O., Whelan, P.F.: Segmentation of the left ventricle of the heart in 3-D+t MRI data using an optimized nonrigid temporal model. IEEE Trans. Med. Imaging 27(2), 195–203 (2008)
9. Fradkin, M., Ciofolo, C., Mory, B., Hautvast, G., Breeuwer, M.: Comprehensive segmentation of cine cardiac MR images. Med. Image. Comp. Comp. Assist. Interv. 11(pt 1), 178–185 (2008)
10. Ben Ayed, I., Lu, Y., Li, S., Ross, I.: Left ventricle tracking using overlap priors. Med. Image. Comp. Comp. Assist. Interv. 11(pt 1), 1025–1033 (2008)
11. Boykov, Y., Jolly, M.P.: Interactive Organ Segmentation Using Graph Cuts. In: Delp, S.L., DiGoia, A.M., Jaramaz, B. (eds.) MICCAI 2000. LNCS, vol. 1935, pp. 276–286. Springer, Heidelberg (2000)

12. Lin, X., Cowan, B., Young, A.: Model-based Graph Cut Method for Segmentation of the Left Ventricle. In: Conf. Proc. IEEE Eng. Med. Biol. Soc., vol. 3, pp. 3059–3062 (2005)
13. Cocosco, C.A., Niessen, W.J., Netsch, T., Vonken, E.J., Lund, G., Stork, A., Viergever, M.A.: Automatic image-driven segmentation of the ventricles in cardiac cine MRI. J. Magn. Reson. Imaging 28(2), 366–374 (2008)
14. Frangi, A.F., Niessen, W.J., Viergever, M.A.: Three-dimensional modeling for functional analysis of cardiac images: a review. IEEE Trans. Med. Imaging 20(1), 2–25 (2001)
15. Otsu, N.: A Threshold Selection Method from Gray-Level Histograms. IEEE Transactions on Systems, Man, and Cybernetics 9(1), 62–66 (1979)
16. Gonzalez, R.C., Woods, R.E.: Digital Image Processing, 2nd edn., ch. 4. Prentice-Hall, New Jersey (2001)
17. http://www.medis.nl/index.htm
18. van Assen, H.C., Danilouchkine, M.G., Frangi, A.F., Ordás, S., Westenberg, J.J., Reiber, J.H., Lelieveldt, B.P.: SPASM: a 3D-ASM for segmentation of sparse and arbitrarily oriented cardiac MRI data. Med. Image Anal. 10(2), 286–303 (2006)
19. Sorgel, W., Vaerman, V.: Automatic heart localization from 4D MRI datasets. SPIE: Med. Imag. 3034, 333–344 (1997)
20. Papavassiliu, T., Kühl, H.P., Schröder, M., Süselbeck, T., Bondarenko, O., Böhm, C.K., Beek, A., Hofman, M.M., van Rossum, A.C.: Effect of endocardial trabeculae on left ventricular measurements and measurement reproducibility at cardiovascular MR imaging. Radiology 236(1), 57–64 (2005)
21. Weinsaft, J.W., Cham, M.D., Janik, M., Min, J.K., Henschke, C.I., Yankelevitz, D.F., Devereux, R.B.: Left ventricular papillary muscles and trabeculae are significant determinants of cardiac MRI volumetric measurements: effects on clinical standards in patients with advanced systolic dysfunction. Int. J. Cardiol. 126(3), 359–365 (2008)
22. Lin, X., Cowan, B.R., Young, A.A.: Automated detection of left ventricle in 4D MR images: experience from a large study. Med. Image Comp. Comp. Assist. Interv. 9(pt 1), 728–735 (2006)